JPNT 9(4), 327-336 (2020)
https://doi.org/10.11003/JPNT.2020.9.4.327

JPNT Journal of Positioning, Navigation, and Timing

Space Service Volume Augmented with Korean Positioning System at Geosynchronous Orbit

Gimin Kim[1], Chandeok Park[1†], Deok Won Lim[2]

[1]Department of Astronomy, Yonsei University, Seoul 03722, Republic of Korea
[2]Navigation R&D Section, Korea Aerospace Research Institute, Daejeon 34133, Republic of Korea

ABSTRACT

This study presents signal availability of inter-operable global navigation satellite system (multi-GNSS) combined with future Korean Positioning System (KPS), specifically at geosynchronous orbit (GSO). The orbit of KPS, which is currently under conceptual feasibility study, is first introduced, and the grid points for evaluating space service volume (SSV) at GSO are generated. The signal observabilities are evaluated geometrically between those grid points and KPS/GNSS satellites. Then, analyzed are the visibility averaged over time/space and outage time to not access one or four signals. The reduction of maximum outage time induced by KPS are presented with different maximum off-boresight angles depending on L1/E1/B1 and L5/L3/E5a/B2 frequencies. Our numerical analysis shows that the SSV of multi-GNSS combined with KPS provides up to 7 additional signals and could provide continuous observation time (zero outage time) of more than four GNSS or KPS signals for 3.20-14.83% of SSV grid points at GSO. Especially at GSO above North/South America and Atlantic region, the introduction of KPS reduces the outage duration by up to 63 minutes with L1/E1/B1 frequency.

Keywords: geosynchronous orbit, Korean positioning system, signal availability, space service volume

1. INTRODUCTION

The regional navigation satellite system (RNSS) such as Indian Regional Navigation Satellite System (IRNSS or NavIC of India) and Quasi-Zenith Satellite System (QZSS of Japan) aims to cooperate with global navigation satellite system (GNSS) to enhance navigation performance, and/or to offer independent navigation services when GNSS's are not available (United Nations 2010). Korean Positioning System (KPS) is currently under feasibility study with conceptual design for the purpose of providing regional navigation service to Korean peninsula and as far as East Asia. Fig. 1 shows the ground tracks of its candidate constellation (Shin et al. 2019), which is composed of three geosynchronous-orbit (GEO) and four inclined-geosynchronous-orbit (IGSO) satellites sharing similar ground tracks; more than four of them are always observable above Korean peninsula, and thus independent navigation service is available.

Meanwhile, the utilization of Space Service Volume (SSV) of inter-operable GNSS (multi-GNSS) can be one of promising solutions to improve the navigation performance at geosynchronous orbit (GSO) in the near future. For accurate mission planning with future GNSS signal availability and power, the SSV of Global Positioning System (GPS) was specified and formal requirements for signal received power, availability and accuracy were established first among other GNSS (Bauer et al. 2006). The definition of multi-GNSS SSV was followed by each GNSS provider and was published as a booklet in United Nations International Committee on GNSS (ICG) working group B (United Nations 2018). It provides the performance of GNSS constellations by three parameters: pseudorange accuracy,

Received Aug 18, 2020 **Revised** Sep 07, 2020 **Accepted** Sep 17, 2020
†**Corresponding Author**
E-mail: park.chandeok@yonsei.ac.kr
Tel: +82-2-2123-5692 Fax: +82-2-392-7680
Gimin Kim https://orcid.org/0000-0002-7576-9565
Chandeok Park https://orcid.org/0000-0002-1616-6780
Deok Won Lim https://orcid.org/0000-0002-5154-8063

Copyright © The Institute of Positioning, Navigation, and Timing

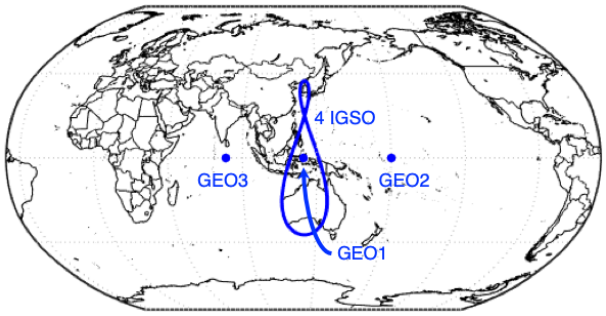

Fig. 1. Ground tracks of Korea Positioning System (KPS) satellites. KPS consists of three geosynchronous (GEO) and four inclined-geosynchronous-orbit (IGSO) satellites. Four IGSO satellites share an almost identical ground-track.

received signal power and signal availability for each GNSS and combined multi-GNSS. While KPS fulfills its primary purpose of providing regional navigation service to Korean peninsula, its prospective signals, which are presumed to be composed of L1/L2/L5 and other frequencies, can be easily compatible for receivers designed for GPS. Therefore, a new definition of KPS SSV is needed to support users who want to utilize additional KPS signals.

This research focuses on the anticipated signal availability of multi-GNSS jointed with virtual KPS at GSO. The signal availability is analyzed in terms of geometric visibility and continuous outage time. We first briefly describe how to formulate geometrical access and present the anticipated enhancement of signal availability both qualitatively and quantitatively.

2. METHODOLOGY

2.1 Geometrical Access Model for Visibility Analysis

GNSS signals have relatively weaker signal strength than other ranging signals of typical satellite tracking system, but they mostly provide wider beam-width to cover the entire Earth in terms of line of sight. As for signal strength, GNSS providers specified their minimum received signal power to be less than -178 decibel-watt (dBW), while the simulated carrier-to-noise-density ratio (C/N_0) is calculated to be less than 25 dB-Hz mostly (United Nations 2018). Therefore, the RF access link budget is critical to determine signal availabilities of KPS. However, in this research, we focus on transmit antenna pattern approximated by geometric angles, as the transmission power of KPS is not yet specified. It is assumed that the minimum received signal powers of KPS are -187 dBW and -184 dBW for L1 and L5 frequencies, respectively, considering that the current weakest minimum received signal powers (defined in United Nations 2018) are from BDS IGSO/GEO satellites (-185.9 dBW for B1 frequency and -184.4 dBW for B3 frequency). The carrier-to-noise density ratio (C/N0) threshold is assumed to 15 dBHz for the purpose of including potential signal acquisition with high gain antenna and low noise amplifier. With these assumptions, the geometrical access model is possible to represent the signal availability of GNSS and KPS. Roughly speaking, the visibility in this study implies no obstacles through the line-of-sight. To determine visibility, we use the antenna off-boresight angle which can be easily calculated when the position vectors of each GNSS satellite and a user satellite are given. The antenna off-boresight angle represents the approximated antenna beam pattern. For example, the maximum off-boresight angle of GPS L1 signal is about 23.5°. The antenna gain of GPS L1 signal at 23.5° off-boresight angle from Block IIR satellites is measured about 1 dB and has side lobe whose gain is at most 4 dB at 30° off-boresight angle (Enderle 2016). In this research, however, these patterns are simplified by bisection for ease of analysis; uniform antenna gain between boresight and maximum off-boresight angle, and zero antenna gain otherwise.

A position vector of a user satellite at the epoch of signal reception denoted as $\vec{r}_{SSV}$ is subtracted from a position vector of a GNSS satellite at the epoch of signal transmission denoted as $\vec{r}_{GNSS}$ to form the line-of-sight vector in Eq. (1). Both epochs are given in GPS time.

$$\vec{\rho} = \vec{r}_{GNSS} - \vec{r}_{SSV} \tag{1}$$

Then, an off-boresight angle α_s, which is an angle between the antenna boresight direction of transmitting antenna of GNSS satellite and the direction of transmitting signal, is calculated by Eq. (2). The antenna boresight direction is often approximated as the nadir direction pointing the Earth center ($\vec{r}_{pt} = [0, 0, 0]^T$) except NavIC.

$$\alpha_s = acos\left[\frac{\vec{r}_{boresight}\cdot(-\vec{\rho})}{|\vec{r}_{boresight}||\vec{\rho}|}\right], \text{ where } \vec{r}_{boresight} = \vec{r}_{pt} - \vec{r}_{GNSS} \tag{2}$$

The off-boresight angles range in $[0, \pi]$. It is assumed that the maximum off-boresight angle of GNSS depicts the main-lobe of transmitting antenna pattern. The transmitting antenna pattern is approximated as uniform antenna gain when the off-boresight angle is less than the pre-specified maximum off-boresight angle. The off-boresight angle of each GNSS signal possesses its maximum value, depending on each constellation and each frequency. If the calculated

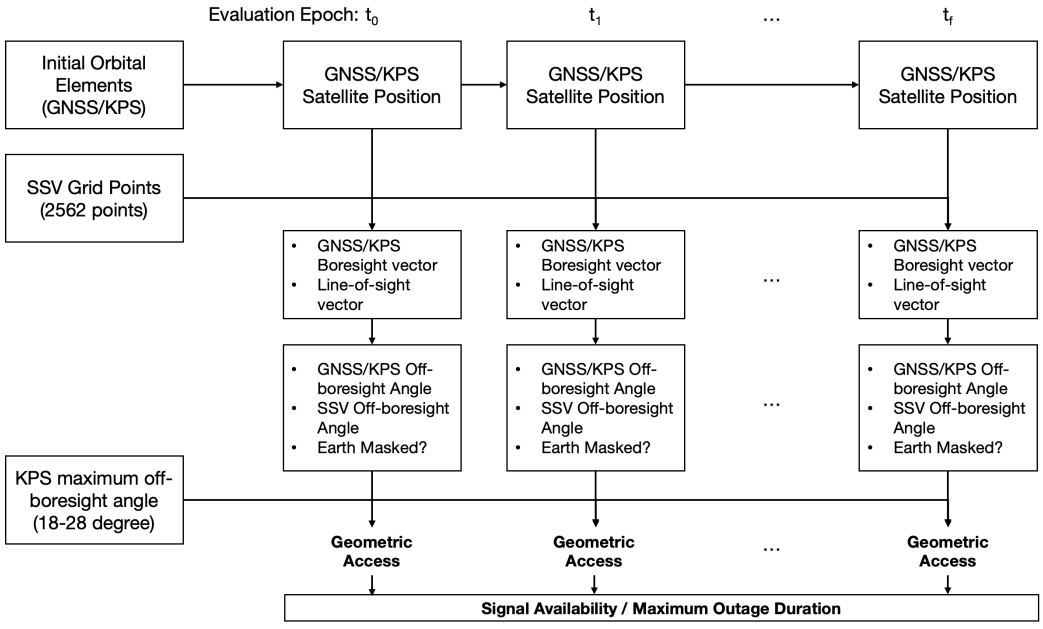

Fig. 2. Simulation process for SSV evaluation using geometric access.

off-boresight angle is beyond the maximum off-boresight angle, the visibility is determined as false (off/invisible) and zero-value is taken into account for signal availability calculation. The maximum off-boresight angle of KPS is used as a simulation parameter to test possible future designs of KPS.

The off-boresight angle is also applicable for the receiver antenna. If the receiving antenna with hemispherical field of view always points the nadir direction, the off-boresight angle of receiver α_{SSV} is calculated by Eq. (3).

$$\alpha_{SSV} = acos\left[\frac{(-\vec{r}_{SSV})\cdot(-\vec{\rho})}{|\vec{r}_{SSV}||\vec{\rho}|}\right] \tag{3}$$

Signal blockage due to Earth is modelled with the off-nadir angle $\alpha_{\oplus}$ of GNSS transmitting antenna:

$$\alpha_{\oplus} = acos\left[\frac{(-\vec{r}_{GNSS})\cdot(-\vec{\rho})}{|\vec{r}_{GNSS}||\vec{\rho}|}\right] \tag{4}$$

Then, the visibility is determined with the following three conditions in Eq. (5):

$$\begin{aligned} &\alpha_s < \alpha_{max} \\ &\alpha_{SSV} < \frac{\pi}{2} \\ &\left|\vec{r}_{GNSS}\right| \sin\alpha_{\oplus} > R_{\oplus} + H \end{aligned} \tag{5}$$

First, the off-boresight angle of GNSS transmitter α_S cannot exceed maximum off-boresight angle α_{max} of specific GNSS considered. Second, the off-boresight angle of receiver α_{SSV} cannot exceed 90°. Finally, the radius of a circle that are tangential to the signal path cannot excced the sum of Earth radius $R_{\oplus}$ and prespecified atmospheric height H.

Table 1. Simulation parameters.

Parameter name	Parameter value
Epoch	2016.01.01 12:00:00 UTC
Duration (minutes)	20,160 (14 days)
Time step (minutes)	1
Number of SSV grid points	2,562
SSV grid altitude (km)	36,000
Antenna boresight direction	GNSS receiver at SSV point: Nadir GNSS transmitter: Nadir except NavIC (5°N 83°E)
Earth radius (km)	6,378
Atmospheric altitude (km)	50

2.2 Simulation of Geometric Access

The overall simulation process for SSV evaluation using geometric access is composed of satellite orbit propagation, SSV grid point generation and access evaluation (Fig. 2). The position of GNSS satellites including KPS is propagated from initial epoch to each evaluation time using two-body equation. The KPS orbital elements at initial epoch are derived from Shin et al. (2019) while GNSS orbital elements at initial epoch are derived from United Nations (2010). Table 1 shows parameters applied in this study. SSV grid points are generated to represent user GSO satellites (Fig. 3). The grids were designed based on icosahedron method (Teanby 2006) such that they represent equal area. Evenly distributed SSV grid points are beneficial to calculating

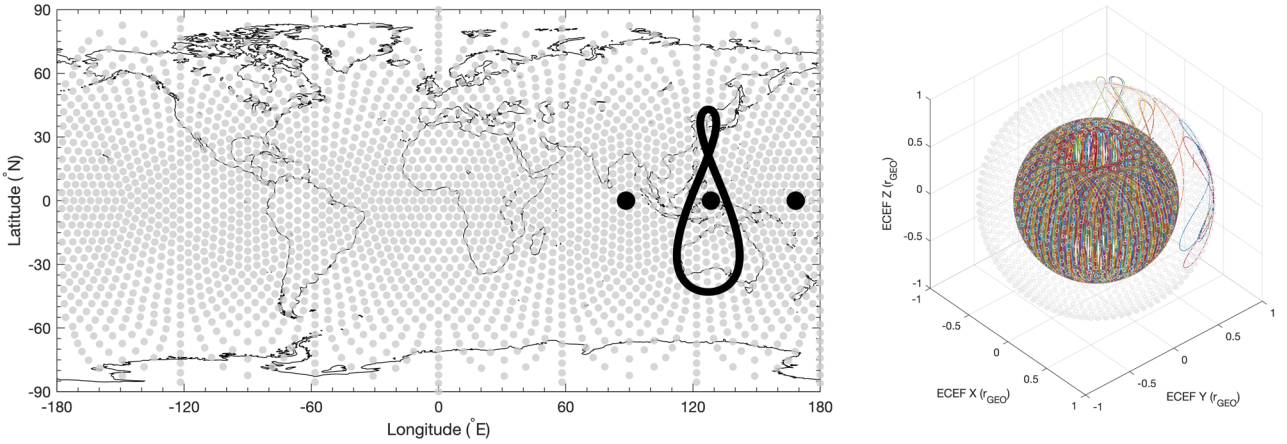

Fig. 3. (Left) Latitude and longitude of SSV grid points in gray dots and ground tracks of KPS satellites in black lines and dots. (Right) Orbits of GNSS and KPS represented in colored lines in ECEF frame in 3 dimensions. Circles in gray color are SSV grid points at GSO altitude. Each axis is normalized by GSO altitude. IGSOs and GEOs of BDS, QZSS, NavIC and KPS satellites are intensively distributed above Asia/Pacific regions.

Table 2. Maximum off-boresight angles (°) for each GNSS constellation.

Spectral band	MEO			IGSO/GEO			
	GPS	GLONASS	Galileo	BDS	BDS	QZSS	NavIC
L1/E1/B1	23.5	20	20.5	25	19	22	N/A
L5/L3/E5a/B2	26	28	23.5	28	22	24	16

unbiased average of signal availability. The grid has roughly 4° spacing near the equator and comprises 2562 points. The geometric access is evaluated from the off-boresight angle calculated from position of each SSV grid point and GNSS/KPS satellites. To investigate the effects of undetermined maximum off-boresight angle of KPS, we evaluated the geometric access augmented with KPS signals depending on the maximum off-boresight angle of KPS.

Time span of simulation is cautiously selected to analyze geometric access in SSV. Satellites at GSO have periods of about one sidereal day. While typical GNSS satellites have periods of around 12-hours, Galileo satellites have the longest periods of 14.08 hours due to their highest altitudes and GLONASS satellites have the shortest periods of 11.26 hours. Furthermore, the shorter the difference of orbital periods, the longer the synodic period of two constellation results. For the same orbital plane, the synodic period of i-th GNSS satellite and arbitrary SSV point at geosynchronous altitude can be approximated as

$$\frac{1}{S} = \frac{1}{P_{GNSS,i}} - \frac{1}{P_{SSV}} \tag{6}$$

For GPS-GLONASS satellites, about 190 hours (7.9 days) of synodic period results from 0.71 hour difference of each orbital period. Hence, the time span of simulation is selected to be 14 days to compensate for the synodic period.

We use two scenarios called Scenarios L1 and L5 to assess the visibility of GNSS signals. Scenario L1 uses L1, L1, E1, B1, and L1 frequency for GPS, GLONASS, Galileo, BDS and QZSS constellations, respectively. Scenario L5 uses L5, L3, E5a, B2, L5, L5 frequency for GPS, GLONASS, Galileo, BDS, QZSS and NavIC constellations, respectively. Each scenario has different maximum off-boresight angles for individual GNSS constellation specified in Table 2 (United Nations 2018). GNSS satellites provide wider maximum off-boresight angles for Scenario L5 compared to Scenario L1, and the maximum off-boresight angles of IGSO/GEO satellites are narrower than those of MEO satellites. The two scenarios are expanded as four scenarios when augmented with KPS, so that they represent L1 and L5 scenarios with/without KPS.

2.3 Figures of Merit

In this study, 'visibility' is used as signal observability from one receiver toward GNSS satellites at one specific epoch. Additionally, 'point signal availability' at one receiver toward multiple GNSS satellites is evaluated with one or more signals. The point signal availability denotes the time average of a series of binary numbers, in which "1" represents that one or more GNSS signals are observable and "0" represents that no GNSS signal is observable at the specific SSV point. 'Global signal availability' is defined as space average of all point signal availabilities at all SSV points.

Maximum outage duration (MOD) is another figure of merit to assess SSV performance, as continuous signal reception is a key to successful GNSS positioning. Outage duration is calculated by detecting consecutive observation arc and summing epochs that does not meet one/four or more signals. Global MOD is defined as space-maximum

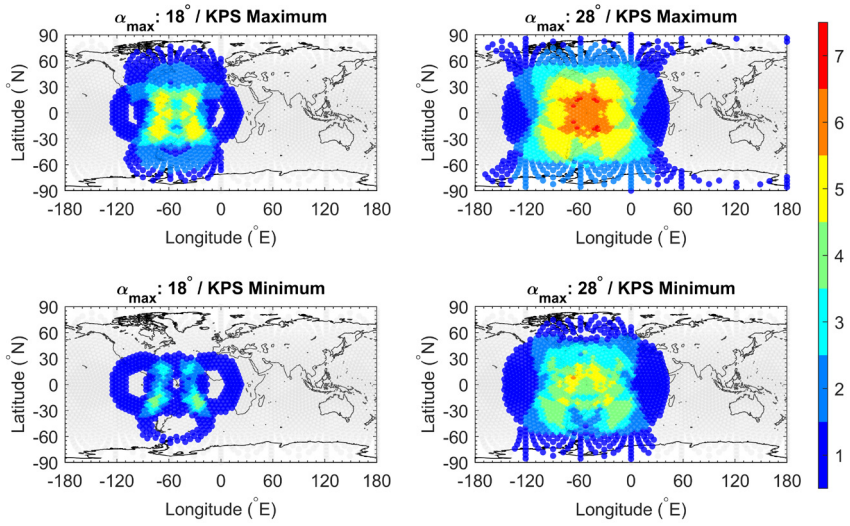

Fig. 4. Maximum/Minimum number of simultaneous KPS signals at each grid point. Gray colored points represent grids of no observable KPS signals.

of MODs at all SSV points. Also, the difference between MOD of GNSS and MOD of GNSS combined with KPS is additional figure of merit to evaluate inter-operable KPS SSV. The subscript *j* in Eq. (5) refers to the number of signals used for criteria; the outage is defined when the number of signals is lower than *j*.

$$\Delta \mathrm{MOD}_j = \mathrm{MOD}_{GNSS,j} - \mathrm{MOD}_{(GNSS+KPS),j} \tag{7}$$

ΔMOD can present the effects of adding KPS signals for specific SSV point. Note that the outage time is calculated in integer minutes, as the simulations are performed with one-minute intervals.

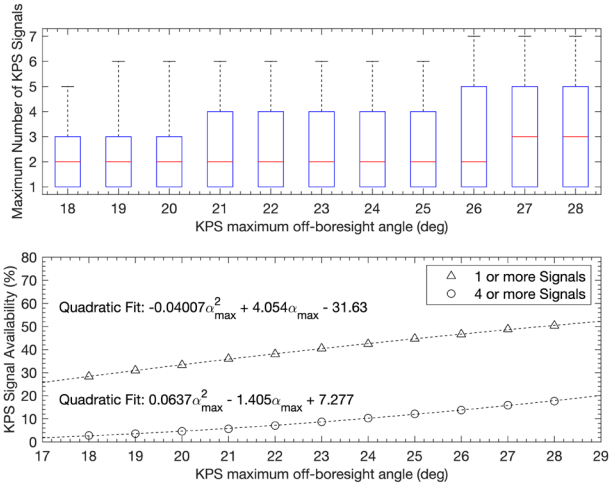

Fig. 5. (Top) Box plot of maximum numbers of available KPS signals at grid points of at least one observable signal. (Bottom) KPS signal availability (%) in GSO altitude vs. maximum off-boresight angle.

3. RESULTS

3.1 KPS Signal Availability

Fig. 4 shows the number of observable KPS signals with respect to two extreme off-boresight angles. The left column of Fig. 4 shows the results with 18° of maximum off-boresight angle. Due to limited ground-track of GSO satellites of KPS, its coverage is limited to regions with longitudes between about 120°W and 30°E. Three GSO satellites of KPS form ring-shaped observable regions at SSV points dominantly near equator, while four IGSO satellites cannot always provide observable regions whose latitudes are higher than about 30°N. Only 17 SSV grid points (corresponding to 0.66% of total SSV grid points) can observe more than four KPS signals for all simulation epochs. The result also shows that 169 (6.60%) and 85 (3.32%) SSV grid points can observe more than 4 and 5 KPS signals at their maximum observability, respectively. The right column of Fig. 4 shows the results with 28° of maximum off-boresight angle. The ring-shaped region appearing in the left column with 18° of maximum off-boresight angle becomes wider with higher visibility between about 150°W and about 50°E. It can be also seen that KPS covers grid points near polar regions with 28° of maximum off-boresight angle. Furthermore, maximum 10 grid points (0.39%) can observe 7 KPS signals simultaneously at some epochs.

The top of Fig. 5 shows the box plot of maximum number of KPS signals at grid points where at least one KPS signal is observed. The red line shows the median value among the maximum numbers. The bottom of Fig. 5 shows the percentage of KPS signal availability from the SSV grids vs.

Table 3. Global signal availability (truncated up to the second decimal) and MOD for scenarios L1 and L5.

Constellation	KPS max. off-boresight angles (°)	Scenario L1				Scenario L5			
		1 signal or more		4 signals or more		1 signal or more		4 signals or more	
		Avail. (%)	MOD (min)	Avail. (%)	MOD (min)	Avail. (%)	MOD (min)	Avail. (%)	MOD (min)
GNSS	-	99.96	39	94.48	96	100	0	99.96	35
GNSS+ KPS	18	99.97	39	94.78	96	100	0	99.96	35
	19	99.97	39	94.84	96	100	0	99.96	35
	20	99.97	39	94.88	96	100	0	99.96	35
	21	99.97	39	94.95	96	100	0	99.96	35
	22	99.97	39	95.00	96	100	0	99.96	35
	23	99.97	39	95.09	96	100	0	99.96	35
	24	99.97	39	95.16	96	100	0	99.96	35
	25	99.97	39	95.26	96	100	0	99.96	35
	26	99.97	39	95.34	96	100	0	99.96	35
	27	99.97	39	95.45	96	100	0	99.96	35
	28	99.97	39	95.53	96	100	0	99.96	35

KPS maximum off-boresight angle. As KPS maximum off-boresight angle becomes larger, KPS signal becomes more available, which can be also seen in Fig. 4. The basic (but efficient) quadratic fittings of signal availability are shown in Eqs. (8) and (9).

$$\mathrm{SA}_1(\%) = -0.04007\alpha_{max}^2 + 4.054\alpha_{max} - 31.63 \tag{8}$$

$$\mathrm{SA}_4(\%) = 0.0637\alpha_{max}^2 - 1.405\alpha_{max} + 7.277 \tag{9}$$

3.2 GNSS Signal Availability / Maximum Outage Duration (MOD)

Under Scenario L1 with GNSS signals only, signal

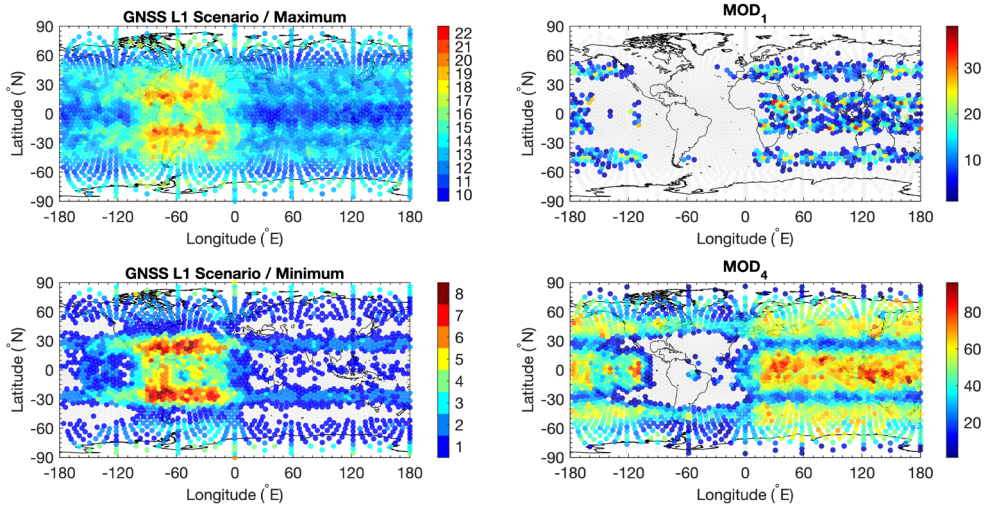

Fig. 6. (Left) Maximum/Minimum number of simultaneous GNSS signals without KPS at each grid point. (Right) Maximum outage duration (MOD) in minutes. Both columns are subject to Scenario L1.

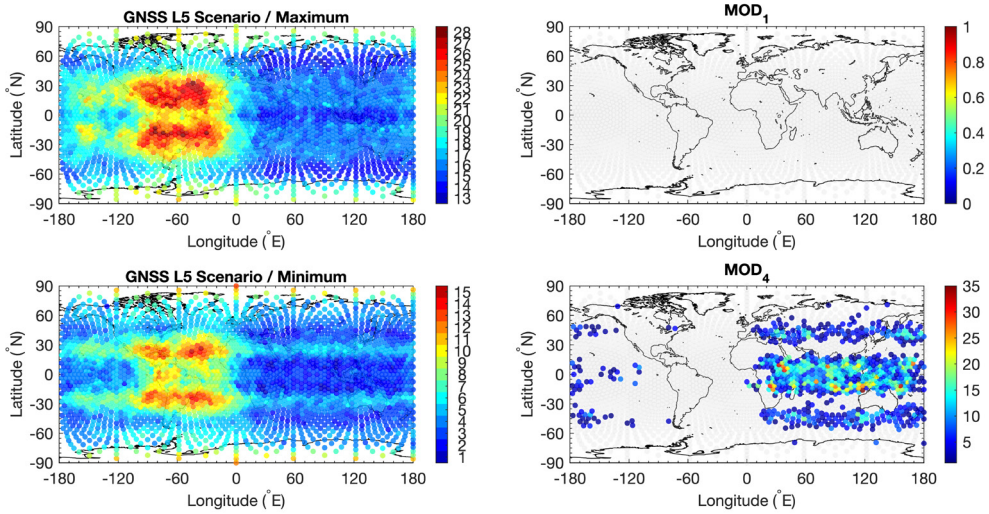

Fig. 7. (Left) Maximum/Minimum number of simultaneous GNSS signals without KPS at each grid point. (Right) Maximum outage duration (MOD) in minutes. Both columns are subject to Scenario L1. Note that all grid points can always observe at least one GNSS signal under Scenario L5, hence no MOD1 on the top right plot.

availability of 1 or more signals is 99.96%, and that of 4 or more signals is 94.48% (Table 3). The left column of Fig. 6 shows the maximum and minimum number of simultaneous GNSS signals in Scenario L1. The number of GNSS signals is not uniformly distributed, but rather centralized in the rectangular region between 120°W and 0°E and between 30°S and 30°N. Also note that there exist grid points whose minimum number of GNSS signals is zero along the equi-latitude line. The right column of Fig. 6 shows MODs. The most notable region is where MOD_4 is zero, which represents no signal outage. Fig. 7 represents the same as Fig. 6, except for Scenario L5. All the grid points can always observe at least one GNSS signal under Scenario L5, resulting in no MOD_1 in the upper right plot. However, MOD_4 still exist in smaller region, the maximum of which is 35 minutes.

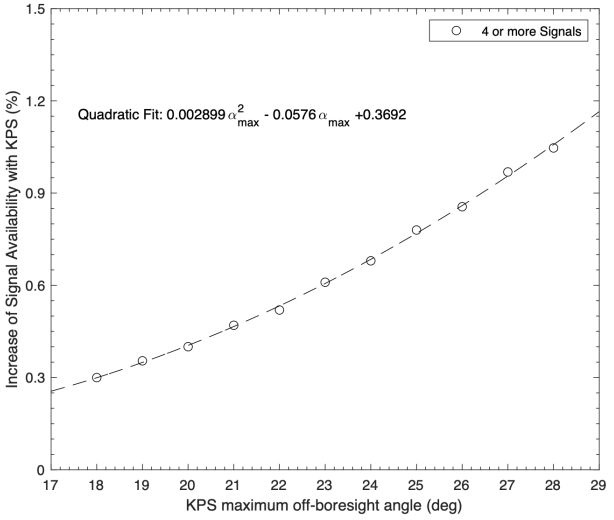

Fig. 8. Increase in global signal availability of KPS-combined GNSS SSV vs. KPS maximum off-boresight angle (Scenario L1).

3.3 KPS-augmented GNSS Signal Availability

A simulation where KPS signals are combined with other GNSS system, i.e., KPS-augmented SSV is conducted in this section. The maximum off-boresight angle of KPS is subject to Scenarios L1 and L5. Table 3 shows the signal availability and MOD with respect to maximum off-boresight angle of KPS. In Scenario L1, global signal availability of 4 or more signals increases about 0.30% – 1.05% by KPS signal augmentation, whereas no prominent changes in Scenario L5 (Fig. 8). MOD, however, shows no changes as those specific grid points showing maximum outage cannot receive KPS signals. In an attempt to examine local effects by KPS augmentation, the grid points affected by KPS are analyzed. Table 4 shows the maximum of ΔMOD and the number of points where MOD decreases with KPS agumentation. Under Scenario L1 with 18°, the reduction of MOD_4 is observed up to 45 minutes in 396 points. However, under Scenario L5 scenario with 18°, the reduction of MOD_4 is observed up to 18 minutes in 22 points.

Fig. 9 shows the location of grid points with ΔMOD greater than zero and the amount of ΔMOD in the combinations of Scenarios L1/L5 and 18°/ 28° of KPS maximum off-boresight angles. The upper row of Fig. 9 shows ΔMOD_1 under Scenario L1. KPS signals contributes to MOD reduction of up to 29 minutes (α_{max} = 18°) and up

Table 4. Maximum ΔMOD and the number of SSV grid points augmented by KPS for Scenarios L1 and L5.

Constellation	KPS max. off-boresight angles (°)	Max. ΔMOD_1 (min)	Max. ΔMOD_4 (min)	No. of ΔMOD_1	No. of ΔMOD_4	No. of points becoming zero outage duration (1 signal) by KPS	No. of points becoming zero outage duration (4 signals) by KPS
Multi-GNSS (L1) + KPS	18	29	45	26 (1.01%)	396 (15.36%)	26 (1.01%)	82 (3.20%)
	19	29	45	35 (1.37%)	459 (17.92%)	34 (1.33%)	103 (4.02%)
	20	29	47	41 (1.60%)	507 (19.79%)	38 (1.48%)	124 (4.84%)
	21	37	47	51 (1.99%)	568 (22.17%)	47 (1.83%)	151 (5.89%)
	22	37	50	60 (2.34%)	616 (24.04%)	55 (2.15%)	169 (6.60%)
	23	37	53	73 (2.85%)	665 (25.96%)	69 (2.69%)	197 (7.69%)
	24	37	54	81 (3.16%)	701 (27.36%)	74 (2.89%)	220 (8.59%)
	25	37	60	96 (3.75%)	752 (29.35%)	91 (3.55%)	253 (9.88%)
	26	37	63	107 (4.18%)	787 (30.72%)	102 (3.98%)	294 (11.48%)
	27	37	63	126 (4.92 %)	842 (32.86%)	121 (4.72%)	334 (13.04%)
	28	37	63	137 (5.35%)	887 (34.62%)	135 (5.27%)	380 (14.83%)
Multi-GNSS (L5) + KPS	18	0	18	0	22 (0.86%)	0	17 (0.66%)
	19	0	18	0	30 (1.17%)	0	20 (0.78%)
	20	0	18	0	33 (1.29%)	0	23 (0.90%)
	21	0	18	0	42 (1.64%)	0	29 (1.13%)
	22	0	18	0	46 (1.80%)	0	32 (1.25%)
	23	0	18	0	58 (2.26%)	0	40 (1.56%)
	24	0	18	0	69 (2.69%)	0	49 (1.91%)
	25	0	24	0	81 (3.16%)	0	58 (2.26%)
	26	0	24	0	90 (3.51%)	0	67 (2.62%)
	27	0	24	0	103 (4.02%)	0	75 (2.93%)
	28	0	24	0	107 (4.18%)	0	79 (3.08%)

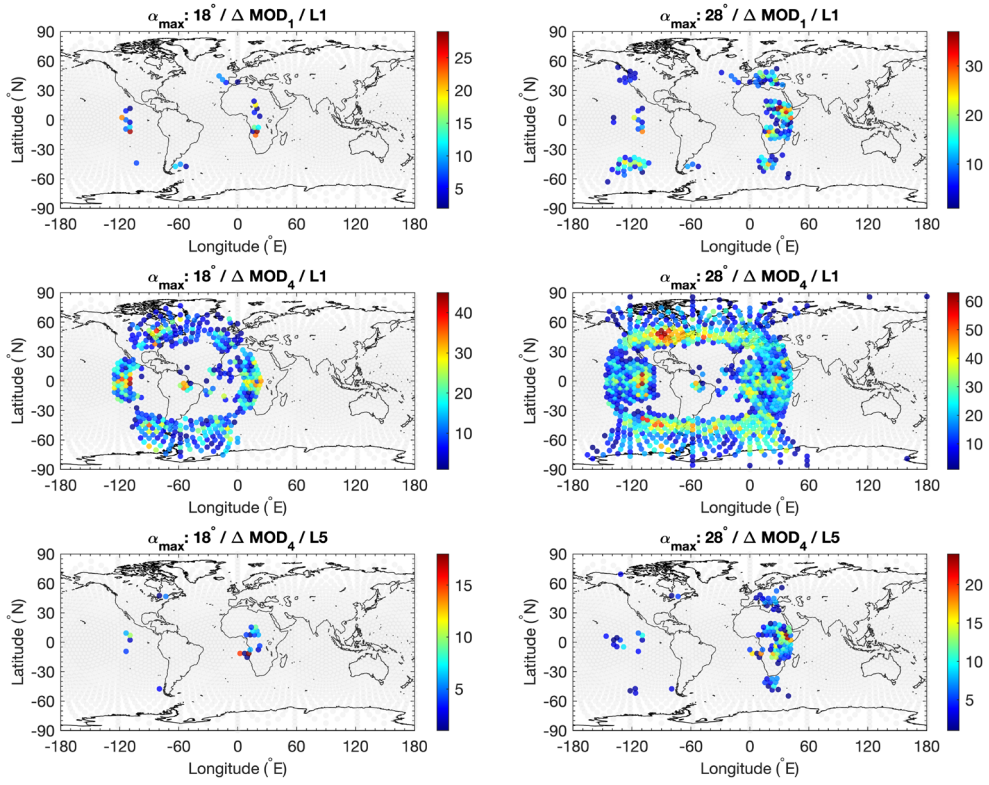

Fig. 9. (Left) Maximum/Minimum number of simultaneous GNSS signals without KPS at each grid point. (Right) Maximum outage duration (MOD) in minutes. Both columns are subject to Scenario L1.

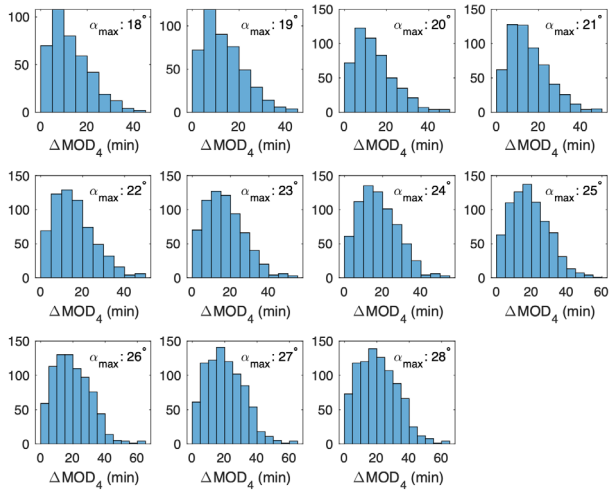

Fig. 10. ΔMOD_4 of Scenario L1 with respect to KPS maximum off-boresight angles. The vertical axis shows the number of SSV points within each 5-minute width bin. SSV points without any MOD change are not included.

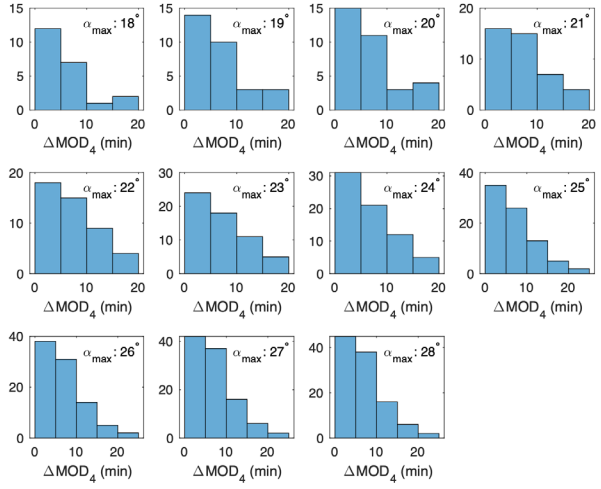

Fig. 11. ΔMOD_4 of Scenario L5 with respect to KPS maximum off-boresight angles. The vertical axis shows the number of SSV points within each 5-minute width bin. SSV points without any MOD change are not included.

to 37 minutes (α_{max} = 28°). However, the spatial distribution is very limited to the grid points above East Pacific, Europe and Africa, because MOD_1 is mostly zero in the center of KPS-visible rergion, as is seen in Fig. 6. The middle row of Fig. 9 shows ΔMOD_4 under Scenario L1. Compared to ΔMOD_1, MOD_4 at each grid point decreases more effectively thanks to KPS. KPS signals reduce MOD up to 45 minutes (α_{max} = 18°) and up to 63 minutes (α_{max} = 28°). The bottom row of Fig. 9 shows ΔMOD_4 under Scenario L5. Compared to Scenario L1, Scenario L5 is subjct to rather small decrease in MOD at each grid point. KPS signals reduce MOD up to 18 minutes (α_{max} = 18°) and up to 24 minutes (α_{max} = 28°).

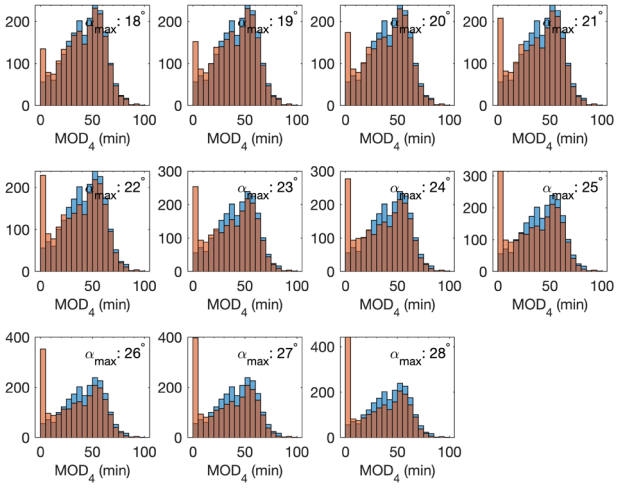

Fig. 12. MOD_4 of Scenario L1 with respect to KPS maximum off-boresight angles. The vertical axis shows the number of SSV points within each 5-minute width bin. Blue and orange bars show the number of SSV points without KPS and with KPS, respectively. SSV points without any MOD change are not included.

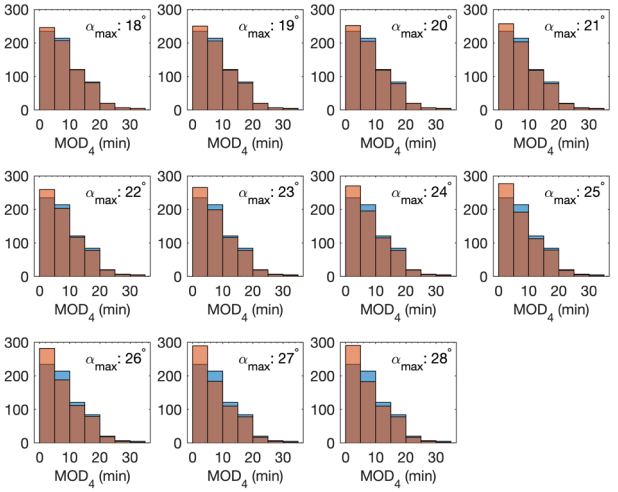

Fig. 13. MOD_4 of Scenario L5 with respect to KPS maximum off-boresight angles. The vertical axis shows the number of SSV points within each 5-minute width bin. Blue and orange bars show the number of SSV points without KPS and with KPS, respectively. SSV points without any MOD change are not included.

All maps of Fig. 9 represent that KPS signal can effectively decrease the amount of outage time not in the region with multiply available KPS signals, but in the region with only one or two available KPS signals at most.

Figs. 10 and 11 show the number of grid points vs. ΔMOD_4 for Scenarios L1 and L5. Each plot shows the result with maximum off-boresight angle of KPS ranging 18° and 28°. Due to abundancy of GNSS signals in Scenario L5, Figs. 10 and 11 show the different number of grid points and different distribution. The absolute MOD values for Scenarios L1 and L5 are also depicted in Figs. 12 and 13. In both figures, zero MOD distribution increases with respect to the maximum off-boresight angle of KPS. Specifically, zero MOD distribution composes more portion than other bins when maximum off-boresight angle of KPS is larger than 22° in Fig. 10. The last two columns of Table 4 show the same results. Under Scenario L1, KPS could provide continuous observation time of more than four GNSS or KPS signals at 3.20-14.83% of SSV grid points at GSO. Meanwhile, under Scenario L5, KPS could provide continuous observation time of more than four GNSS or KPS signals at 0.66-3.08% of SSV grid points at GSO.

4. CONCLUSIONS

In this study, we have analyzed the signal availability and maximum outage duration at GSO for SSV of GNSS combined with KPS. The SSV performance of KPS was investigated with varying maximum off-boresight angles. While the augmentation of KPS in SSV at GSO altitude can provide up to 1% increase of signal availability of more than 4 signals, it can effectively decrease the maximum outage duration of up to 45-63 minutes in Scenario L1 with narrow 18° maximum off-boresight angle. Even though SSV of KPS is overlapped with SSV of former IGSO or GEO satellites from BDS, QZSS and NavIC, KPS is expected to augment the SSV by reducing the outage time to generate position and timing solution. Once the specification of KPS transmit antenna is fixed, more accurate analysis on KPS SSV with tighter constraints of higher threshold of carrier-to-noise-density ratio will be possible, which remains as future work.

ACKNOWLEDGMENTS

This research was supported by a grant from "Fundamental Research for Korea Satellite Navigation System and Future Air Traffic Management" of the Korea Aerospace Research Institute funded by the Korea government (MSIT). This research was also supported by Basic Science Research Program through the National Research Foundation of Korea (NRF) funded by the Ministry of Education (2018R1D1A1B07045759).

AUTHOR CONTRIBUTIONS

Conceptualization, G.K. and C.P.; methodology, G.K. and D.L.; software, G.K.; validation, G.K., C.P. and D.L.; formal analysis G.K., C.P. and D.L.; investigation, G.K.; resources, G.K.; data curation, G.K.; writing—original draft

preparation, G.K.; writing—review and editing, G.K., C.P. and D. L.; project administration, G.K., C.P. and D. L.; funding acquisition, C.P. and D.L.

CONFLICTS OF INTEREST

The authors declare no conflict of interests.

REFERENCES

Bauer, F. H., Moreau, M. C., Dahle-Melsaether, M. E., Petrofski, W. P., Stanton, B. J., et al. 2006, The GPS Space Service Volume, in the 19th International Technical Meeting of the Satellite Division of The Institute of Navigation (ION GNSS 2006), Fort Worth, TX, 26-29 September 2006, pp.2503-2514.

Enderle, W. 2016, ICG SSV – Simulation Phase 2 Link Budget Setup, in ICG 2016 Preparation Meeting, Vienna, 7 June 2016.

Shin, M., Lim, D. W., Chun, S., & Heo, M. B. 2019, A Study on the Satellite Orbit Design for KPS Requirements, JPNT, 8, 215-223. https://doi.org/10.11003/JPNT.2019.8.4.215

Teanby, N. A. 2006, An icosahedron-based method for even binning of globally distributed remote sensing data, Computers & Geosciences, 32, 1442-1450. https://doi.org/10.1016/j.cageo.2006.01.007

United Nations 2010, Current and planned and regional navigation satellite systems and satellite-based augmentations systems, in 2010 International Committee of GNSS, pp.15-40

United Nations 2018, The Interoperable Global Navigation Satellite System's Space Service Volume (Vienna: United Nations Office for Outer Space Affairs)

Gimin Kim is currently M.S. candidate at the Department of Astronomy, Yonsei University in Seoul, Korea. He received his B.S. in Astronomy from Yonsei University in 2018. His research interests cover precise orbit & clock determination of navigation satellites, satellite dynamics, atomic clock modeling, deep-space navigation, remote sensing, etc.

Chandeok Park is a Professor with the Department of Astronomy, Yonsei University in Seoul, Korea. He received his B.S. in Aerospace Engineering from Seoul National University in 1996, M.S. in Aerospace Engineering from Georgia Institute of Technology in 2002, and Ph.D. in Aerospace Engineering from University of Michigan at Ann Arbor in 2006. He worked as a National Research Council Research Associate at Naval Postgraduate School during 2007-2010. His research interests cover precise orbit determination of navigation satellites, deep-space navigation, trajectory design and optimizations for spacecraft formation flying, theoretical/computational optimal controls & optimizations and their applications to spacecraft orbital/interplanetary maneuvers, etc.

Deok Won Lim is a senior research engineer of the Satellite Navigation Team at the Korea Aerospace Research Institute, Korea. He received B.S and Ph.D. degrees from Chungnam National University, Korea, respectively in 2004 and 2011. His current interests include GNSS receiver algorithm, anti-jamming technologies, multipath mitigation techniques and GNSS signal design.